# Modeling and Nonlinear Control of Electric Power Stage in Hybrid Electric Vehicle

Tahri, A.; El Fadil, H.; Guerrero, Josep M.; Giri, F.; Chaoui, F. Z.

*Published in:*
Proceedings of the 2014 IEEE Multi-Conference on Systems and Control (MSC)

*DOI (link to publication from Publisher):*
10.1109/CCA.2014.6981412

*Publication date:*
2014

*Document Version*
Early version, also known as pre-print

# Modeling and Nonlinear Control of Electric Power Stage in Hybrid Electric Vehicle

A.Tahri, H. El Fadil, Josep M. Guerrero, F. Giri, F.Z. Chaoui

***Abstract*— This paper deals with the problem of modeling and controlling the electric power stage of hybrid electric vehicle. The controlled system consists of a fuel cell (FC) as a main source, a supercapacitor as an auxiliary source, two DC-DC power converters, an inverter and a traction induction motor. The proposed strategy involves a multi-loop nonlinear controller designed to meet the three main control objectives: (i) a tight speed regulation in spite of torque load variations. (ii) a good regulation of the DC link voltage; and (iii) a perfect tracking of SC current to its reference. While a Lyapunov based approach is used to control the DC/DC power converters associated with the DC sources, the backstepping technique combined with the field oriented control strategy are invoked in order to control the induction motor. It is formally shown, using a theoretical analysis and simulation results, that the proposed controller meets all the objectives.**

## I. INTRODUCTION

It is widely accepted that the conventional oil production will used up within 20 years (the natural gas production will used up 10–20 years later), while world energy consumption continues to grow at 2% per annum [1], among alternatives is fuel cell fed by hydrogen . Owing to the energy supply problem and environmental problems Proton-exchange-membrane (PEM) fuel cell vehicles have become a major topic of interest in academia and in the automotive industry. A fuel cell system (FCS) has a relatively low power rate as a power source. Moreover, it cannot recover the braking energy. As a result, an FCS alone is not the best solution for the performance of a vehicle; therefore an auxiliary power source is needed [2]. The energy storage system (ESS) can be implemented with either a supercapacitor bank or a rechargeable battery, this work considers the supercapacitor - based ESS.

The major advantage of this technology is that the power-capacity rating of the fuel-cell system is required to meet the average demand only, rather than the peak demand. This makes the fuel cell hybrid system FCHPS more energy efficient than using the fuel cell alone in powering the vehicle. Secondly, rapid load variations may induce oxygen starvation and thereby cause permanent damage to the proton-exchange membranes of the fuel cell. In contrast, the supercapacitor exhibits superior performance in providing peak power, despite its significantly low energy density. Combining an FCS and a supercapacitor bank can provide power system with both high power and energy densities. Thirdly, the FCS generates electric power directly from hydrogen, but a reverse power flow is impossible; the supercapacitor bank therefore provides a reservoir for the regenerative use of electricity [3]. Cell technology demonstrates its high potential in terms of efficiency especially for application in passenger cars, even if many progresses are required for reducing costs and improving reliability in dynamic conditions.

In the other hand, induction motors are suitable for automotive application by their interesting power/mass ratio, relatively low cost and simple maintenance. One of the most popular control strategies of the induction motor is the field-oriented control.

Many works have studied the control of isolated FC-SC DC sources [4], [12] whereas numerous researchers have analyzed control strategies for the association inverter-induction motor [5], [6], [13]-[15].

In the present work, we will develop a new control strategy that simultaneously accounts for all system components *i.e.* the fuel cell source, the supercapacitor, two DC-DC power converters an inverter and a traction motor. The proposed strategy involves a multi-loop nonlinear controller designed to meet the three main control objectives: (i) a tight speed regulation in spite of torque load variations. (ii) a good regulation of the DC link voltage; and (iii) a perfect tracking of SC current to its reference. While a Lyapunov based approach is used to control the DC/DC power converters associated with the DC sources, the backstepping technique combined with the field oriented control strategy are invoked in order to control the induction motor. It will be formally proven that the proposed multi-loop nonlinear controller actually stabilizes the controlled system and meets its tracking objectives.

The paper is organized as follows: in section II, the system studied is presented and modeled, it given a state space representation. In section III, a controller is designed for the whole system and the closed loop system error is analyzed. In section IV, the controller performances are illustrated through numerical simulations. A conclusion and reference list end the paper.

## II. SYSTEM PRESENTATION AND MODELING

### A. System presentation

Figure 1 shows the studied power stage of hybrid electric vehicle (HEV). It includes a hybrid electric storage source which consists of 12.5 KW PEMFC used as the main source and a supercapacitor as auxiliary power source; a boost dc-dc power converter that interfaces the fuel cell with the DC bus; buck-boost converter to interface the supercapacitor in order to store braking energies or to generate peak power during

A.Tahri and F.Z. Chaoui are with the ENSET, Mohamed V University - Souissi, Rabat, 10000, Morocco.

H. El Fadil is with the EISEI Team, LGS Lab. ENSA, Ibn Tofail University, Kénitra, 14000, Morocco (Tel:+212 65 27 68 45; e-mail: h.elfadil@univ-ibntofail.ac.ma, corresponding author).

Josep M. Guerrero is with the Department of Energy Technology, Aalborg University, 9220 Aalborg East, Denmark (Tel: +45 2037 8262; Fax: +45 9815 1411; e-mail: joz@et.aau.dk).

F. Giri is with the GREYC Lab, UMR CNRS, University of Caen Basse-Normandie, 14032, Caen, France.

acceleration; a dc-ac inverter that feds an *7.5 KW* induction motor. All the power converters (dc-dc converters and inverter) operate according to pulse width modulation (PWM) principle.

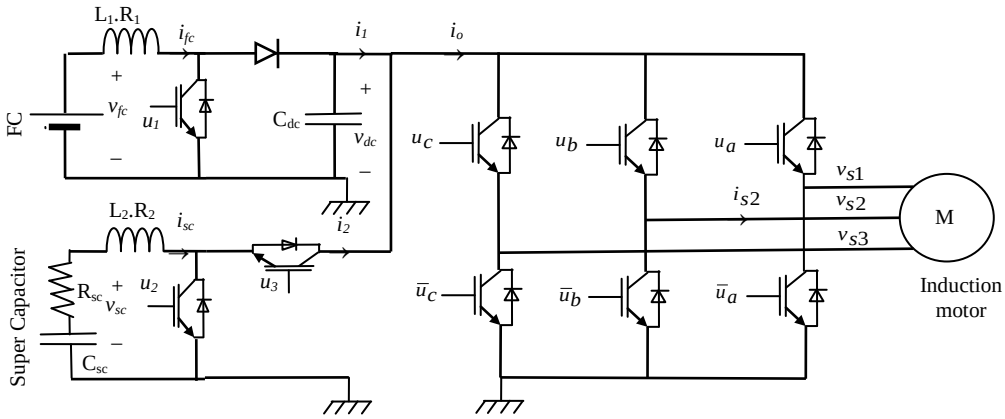


Fig.1: Power stage circuit of hybrid electric vehicle.

*B. Modeling of the DC source subsystem*

From Fig.1 applying Kirchhoff laws one gets the following bilinear switching model of the subsystem consisting of a fuel cell source, a supercapacitor and two dc-dc power converters [4].

$$\frac{di_{fcf}}{dt} = \frac{1}{L_1}(v_{fc} - R_1 i_{fcf} - v_{dc}(1-u_1)) \tag{1a}$$

$$\frac{dv_{dc}}{dt} = \frac{1}{C_{dc}}(i_{fcf}(1-u_1) + u_{23} i_{sc} - i_0) \tag{1b}$$

$$\frac{di_{sc}}{dt} = \frac{1}{L_2}(v_{sc} - v_{dc} u_{23} - R_2 i_{sc}) \tag{1c}$$

$$\frac{dv_{sc}}{dt} = -\frac{i_{sc}}{C_{sc}} - \frac{R_{sc}}{L_2} v_{sc} + \frac{R_{sc}}{L_2} V_{bus} u_{23} \tag{1d}$$

Where $u_{23}$ is the only control input variable of the buck-boost converter defined as follow:

$$u_{23} = k(1-u_2) + (1-k)u_3 \tag{2}$$

where $k$ being a binary variable: $k = 1$ in boost mode and $k = 0$ in buck mode.

*C. Modeling of the inverter-motor association*

In a rotating frame d and q-axis, the induction motor model is described [7]:

$$\frac{di_{sd}}{dt} = ba\phi_{rd} + bp\phi_{rq} - \gamma i_{sd} + \omega_s i_{sq} + m_1 v_{sd} \tag{3a}$$

$$\frac{di_{sq}}{dt} = ba\phi_{rq} - bp\Omega\phi_{rd} - \gamma i_{sq} - \omega_s i_{sd} + m_1 v_{sq} \tag{3b}$$

$$\frac{d\phi_{rd}}{dt} = -a\phi_{rd} + (\omega_s - p\Omega)\phi_{rq} + aM_{sr} i_{sd} \tag{3c}$$

$$\frac{d\phi_{rq}}{dt} = -a\phi_{rq} + (\omega_s - p\Omega)\phi_{rd} + aM_{sr} i_{sq} \tag{3d}$$

$$\frac{d\Omega}{dt} = m(\phi_{rd} i_{sq} + \phi_{rq} i_{sd}) - c\Omega - \frac{1}{J} T_l \tag{3e}$$

$$v_{sd} = u_d v_{dc} \quad , \quad v_{sq} = u_q v_{dc} \tag{3f}$$

where $i_{sd}$, $i_{sq}$, $\varphi_{rd}$, $\varphi_{rq}$, $v_{sd}$, $v_{sq}$, $\Omega$, $T_l$, $u_d$, $u_q$ and $\omega_s$ respectively denote the stator currents, the rotor fluxes, the stator voltage inputs, the angular speed, the load torque, the controls of the inverter and the stator frequency. The subscripts $s$ and $r$ refer to the stator and rotor. The parameters:

$$a = \frac{R_r}{L_r}, b = \frac{M_{sr}}{L_s L_r \sigma}, \gamma = \frac{L_r^2 R_s + M_{sr}^2 R_r}{L_s L_r^2}, m_1 = \frac{1}{L_s \sigma},$$
$$\sigma = 1 - \frac{M_{sr}^2}{L_r L_s}, m = \frac{pM_{sr}}{JL_r}, c = \frac{f_v}{J} \tag{4}$$

where $R_r$ is the rotor resistances, $L_s$ and $L_r$ are the self-inductances of the stator and the rotor, respectively, $M_{sr}$ the mutual inductance between the stator and rotor windings, $p$ the number of pole-pair, $J$ the inertia of the system (motor and load) and $f_v$ the viscous damping coefficient.

Applying a PIPO (Power in equal to Power Out) principle to the inverter one gets:

$$v_{dc} i_0 = i_{sd} v_{sd} + i_{sq} v_{sq} \tag{5}$$

which gives, using (3f):

$$i_0 = u_d i_{sd} + u_q i_{sq} \tag{6}$$

Combining (1), (2), (3) and (5), and using averaging technique [11], the nonlinear averaged model of the whole system is obtained as follows (it is of ninth order)

$$\dot{x}_1 = -\frac{R_1}{L_1} x_1 - (1-\mu_1)\frac{x_2}{L_1} + \frac{1}{L_1} v_{fc} \tag{7a}$$

$$\dot{x}_2 = (1-\mu_1)\frac{x_1}{C_{dc}} + \mu_{23}\frac{x_3}{C_{dc}} - \frac{\mu_d}{C_{dc}}x_5 - \frac{\mu_q}{C_{dc}}x_6 \quad (7b)$$

$$\dot{x}_3 = \frac{x_4}{L_2} - \mu_{23}\frac{x_2}{L_2} - \frac{R_2}{L_2}x_3 \quad (7c)$$

$$\dot{x}_4 = -\frac{x_3}{C_{sc}} - \frac{R_{sc}}{L_2}x_4 + \mu_{23}\frac{R_{sc}}{L_2}x_3 \quad (7d)$$

$$\dot{x}_5 = bax_7 + bpx_9 - \gamma x_5 + \omega_s x_6 + m_1\mu_d x_2 \quad (7e)$$

$$\dot{x}_6 = bax_8 - bpx_7x_9 - \gamma x_6 - \omega_s x_5 + m_1\mu_q x_2 \quad (7f)$$

$$\dot{x}_7 = -ax_7 + (\omega_s - p\Omega)x_8 + aM_{sr}x_5 \quad (7g)$$

$$\dot{x}_8 = -ax_8 + (\omega_s - p\Omega)x_7 + aM_{sr}x_5 \quad (7h)$$

$$\dot{x}_9 = m(x_6x_7 + x_8x_5) - cx_9 - \frac{1}{J}T_l \quad (7i)$$

The control variables are $\mu_1$, $\mu_{23}$, $\mu_{sd}$ and $\mu_{sq}$. whereas the output variables are $x_2$, $x_3$, $x_7$ and $x_9$.

The average values $x_1$ to $x_9$ represent the average values, respectively, of $i_{fc}$, $v_{dc}$, $i_{sc}$, $v_{sc}$, $i_{sd}$, $i_q$, $\phi_{rd}$, $\phi_{rq}$ and $\Omega$. It is worth noting that variables averaging are performed over switching periods. Consequently, the quantities $\mu_1$ and $\mu_{23}$, commonly called duty ratios, vary continuously in the interval $[0\,1]$ and act as the input control signals of dc-dc power converters. Also, the averaged values $\mu_d$ and $\mu_q$ represent the input control signals of the inverter.

## III. Control Design and Analysis

### A. Control objectives

In order to define the control strategy, first one has to establish the control objectives, which can be formulated as follows:

a) Tight regulation of dc-bus voltage;
b) Perfect tracking of SC current to its reference signal;
c) Perfect tracking of rotor speed to its reference profile.

The SC current reference is elaborated by energy management system accordingly to dynamic requirement and FC constraints, as pointed in the introduction.

### B. Controller design for DC-DC power converters.

The first control objective is to enforce the dc bus voltage $v_{dc}$ to track a given constant reference signal $V_{dcref} = 750V$.

However, it is well known that the boost converter has a non-minimum phase feature [10]. Such an issue is generally dealt with by resorting to an indirect design strategy. More specifically, the objective is to enforce the input inductor current $i_{fc}$ to track a reference signal, say $I_{fcref}$. The latter is chosen so that if (in steady state) $i_{fc} = I_{fcref}$ then $v_{dc} = V_{dcref}$, where $V_{dcref} > v_{fc}$. It follows from power conservation consideration, also called PIPO (Power Input equals Power Output), that $I_{fcref}$ is related to $V_{dcref}$ by the relationship

$$I_{fcref} = \lambda_1(V_{dcref}i_o - v_{sc}I_{scref})/\bar{v}_{fc} \quad (8)$$

where $\lambda \geq 1$ being an ideality factor introduced to take into account all losses: switching losses in the converters; the losses in the inductances ESR $R_1$ and $R_2$; the losses in the SC resistance $R_{sc}$.

In order to deal with the two first control objectives, the following errors are introduced

$$e_1 = x_1 - I_{fcref} \quad (9a)$$

$$e_2 = x_2 - x_{2d} \quad (9b)$$

$$e_3 = x_3 - I_{scref} \quad (9c)$$

To stabilize the dc-dc power converters with the state vector $(e_1, e_2, e_3)$, the following control laws are proposed [4]:

$$\mu_1 = 1 - \frac{L_1}{x_2}(c_1e_1 - e_2 + \frac{(v_{fc} - R_1x_1)}{L_1} - \dot{I}_{fcref}) \quad (10a)$$

$$\mu_{23} = 1 - \frac{L_2}{x_2}(c_3e_3 + \frac{(x_4 - R_2x_2)}{L_2} - \dot{I}_{scref}) \quad (10b)$$

where $x_{2d}$ is the desired value of the dc bus voltage $x_2$ and its dynamic is proposed as follows

$$\dot{x}_{2d} = \frac{1}{C_{dc}}(1-\mu_1)x_1 + \mu_{23}x_3 - (\mu_d x_5 + \mu_q x_6) + c_2e_2 + e_1 \quad (10c)$$

Indeed, with these control laws the dynamics of the errors can be obtained as follows:

$$\dot{e}_1 = -c_1e_1 + e_2 \quad (11a)$$

$$\dot{e}_2 = -c_2e_2 - e_1 \quad (11b)$$

$$\dot{e}_3 = -c_3e_3 \quad (11c)$$

The stability of the closed loop system with the state errors $(e_1, e_2, e_3)$ will be investigated in Subsection III-d.

### C. Controller design for the inverter-motor:

The flux field oriented control strategy consists on controlling the rotor flux by $i_{sd}$ current and the electric torque by $i_{sq}$ current. This is possible if $\phi_{rq} = 0$. It is accomplished by realizing:

$$\omega_S = p\Omega + a\frac{M_{sr}}{\phi_{rd}}i_{sq} \quad (12a)$$

Indeed, using (3d) and (12a) one gets $\frac{d\phi_{rq}}{dt} = -a\phi_{rq}$ therefore $\phi_{rq}$ is exponentially vanishing. Therefore, one can suppose that

$$\frac{d\phi_{rq}}{dt} = \phi_{rq} = 0 \quad (12b)$$

The controller design is performed in two steps using the backstepping technique [8]:

*Step1*:

First, we introduce the following tracking errors

$$e_4 = x_7 - \phi_{rd} \tag{13a}$$

$$e_5 = x_9 - \Omega_d \tag{13b}$$

where $\phi_{rd}$ and $\Omega_d$ are the reference signals of the rotor flux and rotor speed, respectively

Deriving (13a-b), it follows from (7g), (7i) and (12a) that:

$$\dot{e}_4 = -ax_6 + aM_{sr}x_5 - \dot{\phi}_{rd} \tag{14a}$$

$$\dot{e}_5 = mx_6x_7 - cx_8 - \frac{T_l}{J} - \dot{\Omega}_d \tag{14b}$$

which suggest the following stabilizing functions

$$x_{5d} = \frac{1}{aM_{sr}}(-c_4e_4 + ax_6 + \dot{\phi}_{rd}) \tag{15a}$$

$$x_{6d} = \frac{1}{mx_7}(-c_5e_5 + cx_7 + \frac{T_l}{J} + \dot{\Omega}_d) \tag{15b}$$

Considering the following intermediates errors

$$e_6 = x_5 - x_{5d} \tag{16a}$$

$$e_7 = x_6 - x_{6d} \tag{16b}$$

One gets, using (7e) and (7f), the following error dynamics

$$\dot{e}_4 = -c_4e_4 + aM_{sr}e_6 \tag{17a}$$

$$\dot{e}_5 = -c_5e_5 + mx_7e_7 \tag{17b}$$

*Step2*:

The objective now is to enforce the error variables $(e_4, e_5, e_6, e_7)$ to vanish. To this end, let us first determine the dynamics of $e_6$ and $e_7$. Deriving (16a) and (16b) and using (7e) and (7f) one obtains

$$\dot{e}_6 = bax_6 - \gamma x_4 + \omega_s x_5 + m_1\mu_{sd}x_3 - \dot{x}_{5d} \tag{18a}$$

$$\dot{e}_7 = bpx_6 - \gamma x_5 - \omega_s x_4 + m_1\mu_{sq}x_3 - \dot{x}_{6d} \tag{18b}$$

The latest equations immediately suggest the following control laws $\mu_{sd}$ and $\mu_{sq}$

$$\mu_{sd} = \frac{1}{m_1x_3}\left(-c_6e_6 - bax_6 + \gamma x_4 - \omega_s x_5 - aM_{sr}e_4 + \dot{x}_{6d}\right) \tag{19a}$$

$$\mu_{sq} = \frac{1}{m_1x_3}\left(-c_7e_7 - bpx_6 + \gamma x_5 + \omega_s x_4 - mx_7e_5 + \dot{x}_{5d}\right) \tag{19b}$$

Finally, combining (18a-b) and (19a-b) one gets

$$\dot{e}_6 = -c_6e_6 - aM_{sr}e_4 \tag{20a}$$

$$\dot{e}_7 = -c_7e_7 - mx_7e_5 \tag{20b}$$

*D. Closed loop stability analysis:*

We are now ready to analyze the stability of the whole closed loop system with the state vector error $e = (e_1, e_2, e_3, e_4, e_5, e_6, e_7)^T$. To this end the dynamics of all errors involved in the control laws (10a-b) and (19a-b) are summarized in the following equations

$$\dot{e}_1 = -c_1e_1 + e_2 \tag{21a}$$

$$\dot{e}_2 = -c_2e_2 - e_1 \tag{21b}$$

$$\dot{e}_4 = -c_4e_4 + aM_{sr}e_6 \tag{21c}$$

$$\dot{e}_5 = -c_5e_5 + mx_7e_7 \tag{21d}$$

$$\dot{e}_6 = -c_6e_6 - aM_{sr}e_4 \tag{21e}$$

$$\dot{e}_7 = -c_7e_7 - mx_7e_5 \tag{21f}$$

Consider the following Lyapunov function candidate

$$V = \frac{1}{2}e^Te \tag{22}$$

Its time-derivative along the trajectories (21a-f) gives

$$\dot{V} = \sum_{i=1}^{7} -c_ie_i^2 \tag{23}$$

which clearly shows that the equilibrium $e$=0 is globally asymptotically stable [9]. The main results of this paper are now summarized in the following proposition:

**Proposition**. Consider the closed-loop system consisting of the power stage of a hybrid electric vehicle represented by (7a-i), (12a) and the controller composed of the control laws (10a-b) and (19a-b). Then, one has:

i) The closed loop system is GAS.
ii) The error $e_1$ converges to zero implying tight dc bus voltage regulation.
iii) The error $e_3$ converges to zero implying perfect tracking of SC current $i_{sc}$ to its reference $i_{scref}$,
iv) The error $e_5$ converge to zero implying that the rotor speed perfectly tracks its reference $\Omega_d$ □

**Proof**.

i) From (22) and (23) one has $V$ positive definite and $\dot{V}$ negative definite which implies that thee equilibrium $e$=0 of the closed loop system with the state vector $e$ is globally asymptotically stable (GAS).
ii) Equation (23) can be rewritten as follows: $\dot{V} \le -2\beta V$, where $\beta = \min_i(c_i)$. Hence, $V$ vanishes exponentially fast, which in turn means, using (22), that the vector error $e$ is exponentially vanishing. The vanishing of the error $e_1$ implies, using (9a) and (8), that the error $x_2 - V_d$ convergence to zero. This, indeed, implies the tight dc bus voltage regulation.
iii) The vanishing of the error $e_3$ implies, using (16), that the SC current $i_{sc}$ perfectly tracks its reference $i_{scref}$.

iv) The vanishing of the error $e_5$ implies, using (13b), that the rotor speed $\Omega$ perfectly tracks its reference $\Omega_d$.

This ends the proof of Proposition ■

The next Section is devoted to the validation of the controller performances.

## IV. Simulation Results:

The performances of the proposed nonlinear control design are illustrated through simulations. The controlled system is simulated with the parameter characteristics listed in Table I.

TABLE I: SYSTEM PARAMETERS

| Element | Its characteristics |
|---|---|
| Fuel cell | 12.5 kW PEMFC, $V_{fcmax}$=900V, $I_{fcmax}$=70A |
| Inductances $L_1$ and $L_2$ | 4.2 mH |
| Inductances ESR: $R_1$ and $R_2$ | 4.2 mΩ |
| Supercapapcitor, $C_{sc}$ | 900F |
| Supercapacitor ESR : $R_{sc}$ | 0.144Ω |
| PWM switching frequency | 10 KHz |

The traction motor is an induction motor of *7.5kW* with the characteristics summarized in Table II. The design parameters are fixed as in Table III. These parameters have been selected using a 'trial-and-error' search method and proved to be suitable.

TABLE II: NUMERICAL VALUES OF CONSIDERED MOTOR CHARACTERISTICS.

| Characteristic | Symbol | Value |
|---|---|---|
| Nominal power | $P_N$ | 7.5 kW |
| Nominal flux | $F_{rn}$ | 1 Wb |
| Nominal voltage | $U_{sn}$ | 0.6 V |
| Stator resistance | $R_s$ | 0.6 Ω |
| Rotor resistance | $R_r$ | 0.5 Ω |
| Number of pole pairs | $p$ | 2 |
| stator self inductance | $L_s$ | 98.3 mH |
| rotor self inductance | $L_r$ | 90 mH |
| Mutual inductance between the stator and rotor windings | $M_{sr}$ | 90 mH |

TABLE III: CONTROLLER DESIGN PARAMETERS

| Parameter | Value |
|---|---|
| $c_1$ | $10^5$ |
| $c_2$ | $10^2$ |
| $c_3$ | $10^2$ |
| Ideality factor $\lambda$ | 1.0004 |

The DC-link voltage reference is set to the constant value $V_{dcref}$ = *750V*. The reference value $I_{scref}$ is set to *-15A*.
The simulations are carried out with following scenario:

- The rotor speed reference is linearly increasing between 0 and 1s (starting mode) (see Fig.3).
- The rotor speed reference is set constant $\Omega_d = 90 rad/s$ between 1s and 3s (see Fig.3).
- At time 2s a load torque is step changing between 30Nm and 60Nm (presence of a slope in the road). (see Fig.3).
- After time 3s the rotor speed reference is linearly decreasing (decelerating mode). (See Fig.3).

Fig. 2 shows that the DC voltage $v_{dc}$ is perfectly regulated to its reference $V_{dcref}$ = 750V. Fig. 3 illustrates that the SC current $i_{sc}$ perfectly tracks its reference $I_{scref}$=*-15V*. This figure also shows that the SC voltage $v_{sc}$ is increasing (charging mode). Fig. 4 illustrate that the rotor speed is regulated to its reference despite the load torque variations.
Finally, Fig.5 and Fig.6 illustrate the control input signals of the dc-dc power converters and the inverter, respectively.

## V. CONCLUSION

The problem of controlling the electric power stage of an electric vehicle combining a hybrid energy storage system and an induction motor has been dressed. The whole system dynamic have been described by the averaged ninth order nonlinear state-space model (7a-i). Based on such a model, the multi-loops nonlinear controller defined by (10a-b) and (19a-b) is designed and analyzed using the Lyapunov approach and the backstepping technique. It is formally proven, using theoretical analysis and simulations results, that the proposed controller achieves all the objectives for which it has been designed for: (i) a tight speed regulation in spite of load torque variations; (ii) a good regulation of the DC Link voltage; and (iii) a perfect tracking of SC current to its reference. This result is confirmed by simulation.

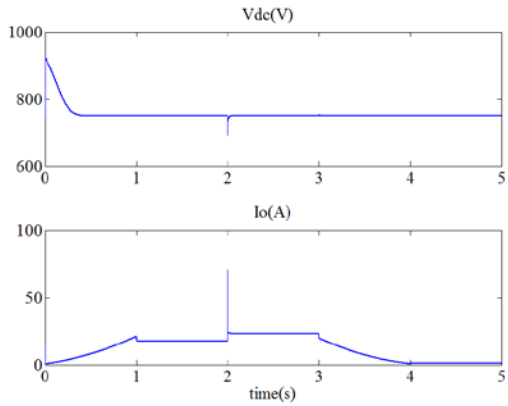


Fig. 2. DC bus voltage and load current in presence of a step voltage refernce $V_{dcref} = 750\,V$, rotor speed reference variations and load torque step changes.

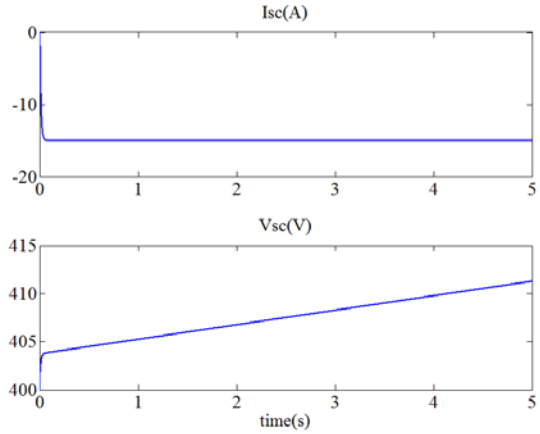


Fig.3: The SC signals in presence of step current refernce $I_{scref} = -15A$ ,

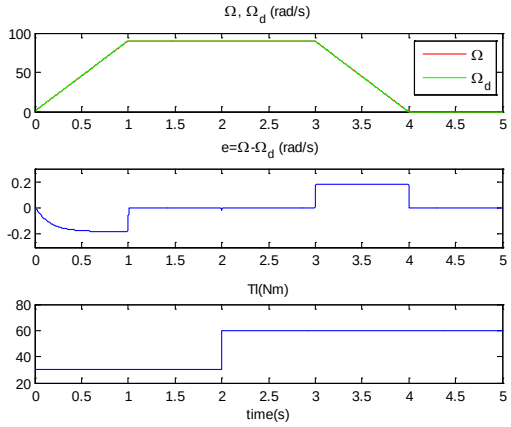


Fig.4: Motor speed tracking capabilies in presence of load torque step changes

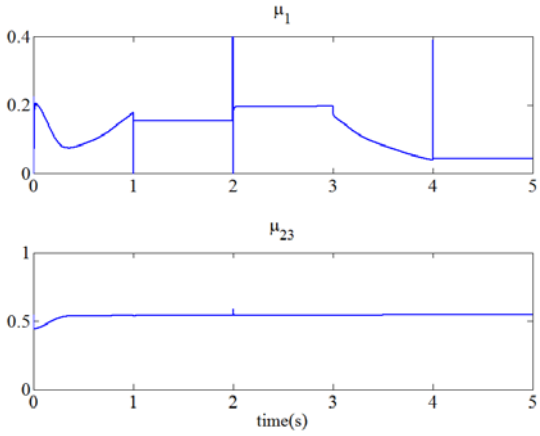


Fig. 5: dc-dc power converters input signals $\mu_1$ and $\mu_{23}$ in presence of rotor speed reference variations and load torque step changes.

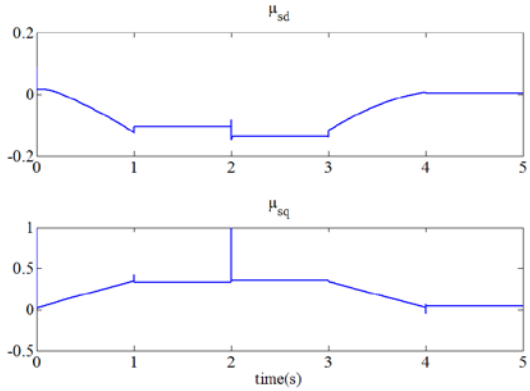


Fig.6: inverter input signals in d-q axis: $\mu_{sd}$ and $\mu_{sq}$ .

## REFERENCES


[1] P. Corbo, F. Migliardini, O. Veneri "Experimental analysis of a 20 kWe PEM fuel cell system in dynamic conditions representative of automotive applications," *Energy Conversion and Management*, 49, pp.2688–2697, 2008.

[2] C. H. Zheng, N. W. Kim, S. W. Cha, "Optimal control in the power management of fuel cell hybrid vehicles". *Int J Hydrogen Energy*; 37(1):655–63, 2012.

[3] W.S. Lin, C.H. Zheng, "Energy management of a fuel cell/ultracapacitor hybrid power system using an adaptive optimal-controlmethod", *Journal of Power Sources* 196 (6), 3280–3289, Mar. 2011.

[4] H. El Fadil, F. Giri, Josep M. Guerrero "Lyapunov based control of hybrid energy storage system in electric vehicles," *American Control Conference* (ACC), 2012 , vol., no., pp.5005-5010, 27-29 June 2012

[5] Yahia K, Zouzou S E, Benchabane F. Indirect vector control of nduction motor with on line rotor resistance identification. *Asian Journal of Information Technology*, 5(12): 1410–1415, 2006.

[6] Ibarra-Rojas, S., Moreno, J., & Espinosa, G. "Global observability analysis of sensorless induction motor". *Automatica*, 40(6), 1079–1085, 2004.

[7] D. Traoré, J. De Leon, A. Glumineaua, "Adaptive Interconnected Observer- Based Backstepping Control Design for Sensorless Induction Motor", *.Automatica*, 48:682-687, 2012.

[8] Krstic M, Kanellakopoulos I, Kokotovic P. *Nonlinear and adaptive control design*. John Willey & Sons, Inc.; 1995.

[9] Khalil H. *Nonlinear systems*. NJ, USA: Prentice Hall; 2003.

[10] El Fadil, H., Giri, F. "Backstepping basedcontrol of PWM DC–DC boost power converters". *In Proc. of the IEEE Int. Symp. on indust. Elect. (ISIE'07*, pp.395–400*)*, 2007.

[11] Krein P.T., Bentsman, J., Bass, R. M., & Lesieutre, B. "On the use of averaging for analysis of power electronic system. *IEEE Transactions on Power Electronics*, 5(2), pp. 182–190, 1990.

[12] P. Thounthong, S. Raël et B. Davat, "Supercapacitors-based on power conditioning for fuel cell automotive hybrid electrical system," *in Proc. 27th Electrical Engineering Conf.* (EECON), Khonkaen (Thaïlande), 11-12 novembre 2004, pp. 497-500.

[13] Khoucha, F.; Lagoun, S.M.; Marouani, K.; Kheloui, A.; El Hachemi Benbouzid, M., "Hybrid Cascaded H-Bridge Multilevel-Inverter Induction-Motor-Drive Direct Torque Control for Automotive Applications," *Industrial Electronics, IEEE Transactions on* , vol.57, no.3, pp.892,899, March 2010.

[14] Garcia, P.; Fernandez, L.M.; Garcia, C.A.; Jurado, Francisco, "Energy Management System of Fuel-Cell-Battery Hybrid Tramway," *Industrial Electronics, IEEE Transactions on* , vol.57, no.12, pp.4013,4023, Dec. 2010.

[15] Zhu, Z.Q.; Howe, D., "Electrical Machines and Drives for Electric, Hybrid, and Fuel Cell Vehicles," *Proceedings of the IEEE* , vol.95, no.4, pp.746,765, April 2007